NIH Public Access
Author Manuscript
Glia. Author manuscript; available in PMC 2008 September 25.

Published in final edited form as:
Glia. 2006 April 1; 53(5): 516–528. doi:10.1002/glia.20312.

Functional Expression of K_{ir}4.1 Channels in Spinal Cord Astrocytes

M.L. OLSEN, **H. HIGASHIMORI**, **S.L. CAMPBELL**, **J.J. HABLITZ**, and **H. SONTHEIMER***
1*Department of Neurobiology and Civitan International Research Center, University of Alabama at Birmingham, Birmingham, Alabama*

Abstract

Spinal cord astrocytes (SCA) have a high permeability to K^+ and hence have hyperpolarized resting membrane potentials. The underlying K^+ channels are believed to participate in the uptake of neuronally released K^+. These K^+ channels have been studied extensively with regard to their biophysics and pharmacology, but their molecular identity in spinal cord is currently unknown. Using a combination of approaches, we demonstrate that channels composed of the K_{ir}4.1 subunit are responsible for mediating the resting K^+ conductance in SCA. Biophysical analysis demonstrates astrocytic K_{ir} currents as weakly rectifying, potentiated by increasing $[K^+]_o$, and inhibited by micromolar concentrations of Ba^{2+}. These currents were insensitive to tolbutemide, a selective blocker of K_{ir}6.x channels, and to tertiapin, a blocker for K_{ir}1.1 and K_{ir}3.1/3.4 channels. PCR and Western blot analysis show prominent expression of K_{ir}4.1 in SCA, and immunocytochemistry shows localization K_{ir}4.1 channels to the plasma membrane. K_{ir}4.1 protein levels show a developmental upregulation in vivo that parallels an increase in currents recorded over the same time period. K_{ir}4.1 is highly expressed throughout most areas of the gray matter in spinal cord in vivo and recordings from spinal cord slices show prominent K_{ir} currents. Electrophysiological recordings comparing SCA of wild-type mice with those of homozygote K_{ir}4.1 knockout mice confirm a complete and selective absence of K_{ir} channels in the knockout mice, suggesting that K_{ir}4.1 is the principle channel mediating the resting K^+ conductance in SCA in vitro and in situ.

Keywords

inward rectifier potassium channel; potassium buffering; astrocyte; knockout; spinal cord

INTRODUCTION

It is widely accepted that astrocytes have an unusually high permeability for K^+ ions (Kuffler and Potter, 1964), which gives rise to a very hyperpolarized resting membrane potential (Kuffler, 1967; Ransom and Goldring, 1973). Many studies have characterized the underlying K^+ channels in astrocytes from different brain regions and different animal species. These studies provide convergent evidence that astrocytes express inwardly rectifying potassium (K_{ir}) channels that have a high open probability near the K^+ equilibrium potential. These channels are thought to aid in potassium redistribution following neuronal activity, a process termed K^+ buffering in the brain (Orkand et al., 1966; Newman, 1984) or K^+ siphoning in the retina (Newman, 1985).

*Correspondence to: Harald Sontheimer, Department of Neurobiology and Civitan International Research Center, University of Alabama at Birmingham, 1719 6th Ave. S., CIRC 545, Birmingham, AL 35294. E-mail: sontheimer@uab.edu

NIH-PA Author Manuscript
NIH-PA Author Manuscript
NIH-PA Author Manuscript

NIH-PA Author Manuscript

NIH-PA Author Manuscript

NIH-PA Author Manuscript

The K_{ir} channel family is composed of 16 cloned subunits, of which several have been identified in astrocytes at the gene or protein level (for review, see Olsen and Sontheimer, 2004). It is unclear which of these genes gives rise to functional channels in astrocytes and participate in the membrane K^+ conductance. In retinal Müller (glial) cells from a transgenic mouse with homozygotic deletion of $K_{ir}4.1$ subunit, K^+ conductance was reduced and cells were depolarized relative to wild-type littermates (Kofuji et al., 2000). This and additional studies in the $K_{ir}4.1$ knockout animal suggest that this subunit is responsible for inwardly rectifying potassium currents in Müller cells (Neusch et al., 2001; Marcus et al., 2002). This subunit has been given a great deal of attention in astrocytes from other brain regions; however, its presence or the lack thereof has not yet been directly coupled to functional currents. In acute hippocampal slices, single-cell polymerase chain reaction (PCR) from astrocytes with prominent inward currents demonstrated very few cells contained transcripts encoding $K_{ir}4.1$, but instead contained transcripts for $K_{ir}2.1$, 2.2, and 2.3 (Schroder et al., 2002). Additionally, a direct comparison between cultured cortical and SCA displayed very different and distinct inward currents, suggesting that different channels are responsible for mediating these currents (Guatteo et al., 1996). These studies suggest the heterogeneity of astrocytic inward currents in different brain regions, necessitating a preparation-specific investigation.

We have used the rat spinal cord as a model system to characterize K_{ir} channels in astrocytes in vitro and in situ. We chose the spinal cord since the continuous propagation of action potentials through the cord produces a high extracellular K^+ load in this structure (Sykova, 1987). If astrocytes are involved in regulating this K^+ load, one might expect particularly prominent expression of K_{ir} channels that participates in the process. Indeed, we have demonstrated robust K_{ir} currents in cultured SCA as well as acute spinal cord slices (Ransom and Sontheimer, 1995; Bordey and Sontheimer, 1998a). K_{ir} channel activity correlates positively with cell differentiation (Ransom and Sontheimer, 1995) and is decreased following injury (MacFarlane and Sontheimer, 1997), as well as in diseases that present with gliosis (Bordey and Sontheimer, 1998b; Bordey et al., 2001).

In this study, we set out to identify the underlying channels in SCA using a number of specific molecular and genetic tools that have become recently available. We demonstrate here that K_{ir} currents in SCA in both rat and mouse are largely, if not solely, attributed to $K_{ir}4.1$.

MATERIALS AND METHODS

Cell Culture and Slice Preparation

Experiments were performed on Sprague-Dawley rats and were approved by the University of Alabama Institutional Animal Care and Use Committee. For culture experiments postnatal day 0 (P0) pups were decapitated. The spinal cords were dissected into ice-cold serum-free EMEM (Gibco, Grand Island, NY) containing 20 mM glucose. Meninges were stripped and cords were minced and placed into an O_2 saturated papain solution (Worthington, Lakewood, NJ) for 20 min. The tissue was washed twice with spinal cord astrocyte media (EMEM supplemented with 10% fetal calf serum (FCS), 20 mM glucose, and penicillin/streptomycin) and then triturated. Cells were plated at a density of 1.0×10^6 cells/ml on polyornithine- and laminin-coated coverslips (12-mm round No. 1, Macalaster Bicknell, New Haven, CT). The media was changed every day for the first 3 days and then every fourth day thereafter. Mature or differentiated SCA (>6 days in culture [DIC]) were used for all cultured experiments (Olsen and Sontheimer, 2004b). For slice experiments, P13-P19 pups were deeply anesthetized with ketamine (100 mg/kg) and perfused with ice-cold saline before the spinal cord was removed. The cord was placed in liquid low melt agar at ~35°C, which was quickly solidified by being placed on ice. Sections from the cervical, thoracic and lumbar regions were cut at 250 μm using a Vibratome (Ted Pella, Redding CA) in ice-cold artificial cerebrospinal fluid (ACSF) (in mM), NaCl 116, KCl 4.5, $MgCl_2$ 0.8, $NaHCO_3$ 26.2, glucose 11.1, HEPES 5.0, which was

NIH-PA Author Manuscript

NIH-PA Author Manuscript

NIH-PA Author Manuscript

continuously bubbled with 5% CO_2. Before recording, slices were allowed to recover for at least 1 h at room temperature in ACSF.

Culture and Slice Electrophysiology

Whole-cell voltage-clamp recordings were obtained via standard methods (Hamill et al., 1981). Patch pipettes were made from thin-walled (outer diameter 1.5 mm, inner diameter 1.12 mm) borosilicate glass (TW150F-4) WPI, Sarasota, FL) and had resistances of 4–6 MΩ when filled with standard KCl pipette solution containing (in mM) 145 KCl, 1 $MgCl_2$, 10 EGTA, 10 HEPES sodium salt, pH adjusted to 7.3 with Tris-base. $CaCl_2$ (0.2 mM) was added to the pipette solution just before recording, resulting in a free calcium concentration of 1.9 nM. Cultured cell recordings were made on the stage of an inverted Nikon Diaphot microscope equipped with Hoffman Modulation Contrast Optics. Current recordings were obtained with an Axopatch 200A amplifier (Axon Instruments, Foster City, CA). Current signals were low-pass filtered at 2 kHz and digitized on-line at 10–20 kHz using a Digidata 1200 digitizing board (Axon Instruments). Data acquisition and storage were conducted with the use of pClamp 8.2 (Axon Instruments). Resting membrane potentials, cell capacitances and series resistances were measured directly from the amplifier, with an upper limit for series resistance of 10 MΩ and series resistance compensation adjusted to 80% to reduce voltage errors. Cultured cells were continuously perfused with a bathing solution containing (in mM) 125 NaCl, 5.0 KCl, 1.0 $CaCl_2$, 10.5 glucose, and 32.5 Hepes. The pH of this solution was adjusted to 7.4 with NaOH and the osmolarity was ~300 mOsm. For the 20 and 50 mM high K^+ solutions, NaCl was replaced with equimolar concentrations of KCl. Drugs were added directly to these solutions. Unless stated otherwise, all drugs were purchased from Sigma (St. Louis, MO). Tertiapin was purchased from Alomone Laboratories (Jerusalem, Israel). For slice recordings, slices were transferred after the recovery period to a Zeiss Axiskop FS microscope (Zeiss, Thornwood, NY) equipped with Nomarski optics, a 40 × water immersion lens and infrared (IR) illumination was used to visualize glia cells in the spinal cord slice. Slices were continuously superfused with ACSF with the addition of 1.8 mM $CaCl_2$. Signals were acquired using an Axopatch 1B amplifier (Axon Instruments, Foster City, CA) controlled by Clampex 9.0 software via a Digidata 1200B interface (Axon Instruments). Signals were filtered at 2 kHz, digitized at 5 kHz. Data acquisition and storage were conducted with the use of pClamp 9.0 (Axon Instruments). Resting membrane potentials and cell capacitances were read directly from pClamp software.

RT-PCR

mRNA was isolated from cultured SCA (>9 DIC) using the RNAqueous kit from Ambion (Austin, TX). To remove contaminating DNA from the mRNA preparation, a DNA removal kit, DNA-free (Ambion), was used. RTPCR was performed using a Qiagen One Step RT-PCR Kit (Valencia, CA). The Qiagen protocol was followed. An Eppendorf Mastercylcer Gradient Thermo Cycler was used (Hamburg, Germany) with an annealing temperature of 60°C for 35 cycles. When possible, published primer sets were used; all other primers were designed using Vector NTI software (Table 1). All primers were manufactured by Invitrogen (Carlsbad, CA). For a positive control, a rat brain cDNA library was used (BD Biosciences, Palo Alto, CA). In the negative control, the sample was set on ice during the initial reverse transcription reaction; *Kcnj10* (K_{ir}4.1 primers) were used in these reactions. In the second negative control, water was substituted for mRNA.

Western Blot Analysis

Cultured dells were lysed using RIPA buffer (50 mM Tris-Cl, pH 7.5, 150 mM NaCl, 1% Nonidet P-40 (NP-40), 0.5% sodium deoxycholate, 1% sodium dodecyl sulfate) for 30 min supplemented with a protease and phosphatase inhibitor cocktail obtained from Sigma (St.

NIH-PA Author Manuscript

NIH-PA Author Manuscript

NIH-PA Author Manuscript

Louis, MO). Cells were sonicated for 10 s, and the homogenates were centrifuged for 5 min at 12,000*g* at 4°C. For whole cords, tissue was minced (<2 mM) and mechanically homogenized in homogenization buffer (10 mM Tris, 1 mM glucose, 5 mM $CaCl_2$) supplemented with protease and phosphatase inhibitors. Protein quantification was performed on the supernatant using a DC protein assay kit from Bio-Rad (Hercules, CA). Protein was heated to 70°C in Laemmli- sodium dodecyl sulfate sample buffer containing 600 mM β-mercaptoethanol for 5 min. Equal amounts of protein were loaded into each lane of a 4–20% gradient pre-cast SDS-gel (Bio-Rad). Proteins were separated at 120 V constant. Gels were transferred onto PVDF paper (Millipore, Bedford, MA) at 200 mA constant for 2 h at room temperature, and these membranes were blocked in blocking buffer overnight. (Santa Cruz Biotechnology, Santa Cruz, CA). The $K_{ir}4.1$ antibody was obtained from Alomone (Jerusalem, Israel) and diluted according to the manufacturer's instructions. Blots were incubated for 90 min at room temperature. The membranes were then rinsed three times for 15 min and incubated with horseradish peroxidase (HPO)-conjugated secondary antibody for 60 min at room temperature. Blots were again washed three times for 10 min and developed with enhanced chemiluminescence (ECL; Amersham, Arlington Heights, IL) on Hyper-film (Amersham). Actin and secondary HRP-conjugated antibodies were purchased from Sigma.

Immunocytochemistry and Immunohistochemistry

Cells plated on coverslips were washed two times with phosphate-buffered saline (PBS) and fixed with 4.0% paraformaldehyde for 15 min. Cells were then washed twice with PBS and then blocked in PBS, 0.3% Triton X-100, and 10% goat serum (blocking buffer, BB) for 30 min. Primary K_{ir} antibodies and anti-glial fibrillary acidic protein (GFAP; Chemicon, Temecula, CA) were diluted in incubation buffer (IB, diluted 1:3 BB) and added, according to the manufacturer's suggestion, overnight at 4°C. The cells were washed three times in PBS before adding a fluorescein isothiocyanate- (FITC) and/or tetramethyl rhodamine isothiocyanate (TRITC)-conjugated secondary antibody (Molecular Probes, Eugene, OR) diluted at 1:500 in IB for 1 h at room temperature. Cells were washed twice with PBS, washed once with 4′-6-diamidino-2-phenylindole (DAPI, 10^{-4} mg/ml, Sigma) diluted in PBS for 5 min. DAPI was rinsed off with PBS, and cells were mounted onto microscope slides with Gel/Mount (Biomedia, Foster City, CA). Fluorescent images were acquired with a Zeiss Axiovert 200M (München, Germany).

Acute spinal cord slices were obtained from postnatal day 15–19 (P15–19) Sprague-Dawley rats. Animals were deeply anesthetized with a peritoneal injection of ketamine (100 mg/kg) and perfused with a 4% paraformaldehyde solution for ~15 min. The whole spinal cord was removed and stored overnight in 4% paraformaldehyde. After washing in PBS, the cord was removed from the column; 50-μm sections were cut using a Vibratome (Oxford Instruments) from the mid-cervical and thoracic regions. Sections were blocked for 1 h in 10% horse serum and 0.3% Triton X-100 in PBS. Antibodies against GLT-1, Neu-N, and MAP-2 were obtained from Chemicon. The following day, the sections were washed three times with IB before being incubated with FITC- or TRITC-conjugated secondary antibodies obtained from Molecular Probes for 60 minutes at room temperature. Slices were then washed twice with IB and twice with PBS before being mounted onto slides. Fluorescent images were acquired with a Zeiss Axiovert 200M (München, Germany).

Transfection of shRNA into Cultured Rat Spinal Cord Astrocytes

A $pK_{ir}4.1$-OFF EGFP was constructed by ligating annealed oligonucleotides GATCCCCGCTCTTCTCGCCAACCTTTACTTCAAGAGAGTAAAGGTTGGCGAGAA GAGCTTTTTA and AGCTTAAAAAGCTCTTCTCGCCAACCTTTACTCTCTTG-AAGTAAAGGTTGGCGAGAAGAGC at *Bgl*II and *Sal*I restriction sites of the pZOFF- EGFP plasmid (Terry-Lorenzo et al., 2005). The small hairpin RNA (shRNA) was targeted to the rat

NIH-PA Author Manuscript

NIH-PA Author Manuscript

NIH-PA Author Manuscript

K_{ir}4.1 cDNA sequence position 314–335. Freshly dissected SCA were transfected with either pZ-OFF EGFP (control) or pK_{ir}4.1-OFF EGFP using Rat Astrocyte Nucleofector Kit (Amaxa, Gaithersburg, MD). Briefly, 2×10^6 cells obtained from P0 rat spinal cords were mixed with 2 μg of pK_{ir}4.1-OFF EGFP or pZOFF EGFP (as negative control) in 100 μl of the nuclear factor solution and then electroporated with the Nucleofector (Amaxa). Electroporated cells were immediately resuspended and plated as described above.

K_{ir}4.1 Knockout Genotyping

The methods used have been previously described with slight modification (Kofuji et al., 2000). P0 *Kcnj10* (K_{ir}4.1) mouse genomic DNA template was obtained by tail clipping. The clipped tail (3 mm) was digested with 50 mM NaOH solution for 10 min at 95°C, vortexed, and neutralized with 1 M Tris (pH 8.0). This was followed by centrifugation for 6 min at 10,000*g*. Primers used for mouse PCR amplification were previously described (Kofuji et al. 2000). K_{ir}4.1 forward 5′-TGG ACG ACC TTC ATT GAC ATG CAG TGG-3′, reverse 5′CTT TCA AGG GGC TGG TCT CAT CTA CCA CAT-3′ and the neomycin resistance gene, forward 5′-GAT TCG CAG CGC ATC GCC TTC TAT C-3′ were used. The PCR protocol described above was used to amplify the gene products. The expected product obtained from wild-type (+/+) allele was 643 bp, while the knockout (-/-) mutant allele produced a 383-bp fragment and finally, the heterozygous (+/-) allele produced both 643- and 383-bp fragments. Once the genotype was established, wild-type and homozygous knockout astrocytes were obtained and cultured separately as described above.

Statistical Analysis

Current responses to varied voltage steps and ramps were analyzed and measured in Clampfit (Axon Instruments); the resulting raw data were graphed and plotted in Origin 6.0 (MicroCal, Northampton, MA). Unless otherwise stated, all values are reported as mean ± SE, with n indicating the number of cells sampled.

RESULTS

K_{ir} channels are responsible for the astrocytic resting conductance

Mature or differentiated cultured SCA express robust inwardly rectifying K_{ir} currents that activate at hyperpolarized potentials and show time- and voltage-dependent inactivation at voltages more negative than -100 mV (Ransom and Sontheimer, 1995). Additionally, K_{ir} currents in SCA are highly sensitive to extracellular Ba^{2+} and increase significantly in higher $[K^+]_o$, as illustrated in a representative example (Fig. 1A). Single-channel analysis has demonstrated a high open probability (0.8–0.9) at the potassium equilibrium potential or the resting membrane potential of SCA (Ransom and Sontheimer, 2005). We set out to demonstrate that the K_{ir} channels we are investigating indeed account for most of the resting conductance and are critical in maintaining the hyperpolarized resting membrane potential (RMP). We obtained whole-cell, patchclamp recordings from cultured SCA and elicited a 40-mV voltage step from a holding potential of -80 mV, a potential close to the resting potential of these cells. Such steps were applied at a frequency of ~5 Hz, while we altered extracellular potassium, $[K^+]_o$, in either the absence or presence of 100 μM Ba^{2+}. The representative recording shown in Figure 1B demonstrates a negative shift in the holding current associated with a greater than three-fold increase in current amplitude when $[K^+]_o$ was increased from 5 mM to 20 mM (Fig. 1C). When the solution was returned to 5 mM $[K^+]_o$ both the holding current and current amplitude returned to baseline. Increasing $[K^+]_o$ to 50 mM elicited an even greater shift in holding current as well as a five-fold increase in current amplitude (Fig. 1B,C). Both responses returned to baseline when switched back to control $[K^+]_o$ (Fig. 1B). Essentially all of the current in control solutions and any increase in current amplitude with increased $[K^+]_o$ were completely eliminated in the presence of Ba^{2+} (Fig. 1C, n = 5). Additionally, Ba^{2+} application caused an

NIH-PA Author Manuscript

NIH-PA Author Manuscript

NIH-PA Author Manuscript

increase in input resistance by almost 20-fold from a mean value of 24.2 ± 7.9 mΩ to 549.5 ± 116.6 MΩ (Fig. 1D, n = 4), indicating that Ba^{2+}-sensitive channels were indeed active at rest and accounted for the majority of the cells resting conductance. To support this conclusion further, we also performed current-clamp experiments in which application of Ba^{2+} in 5 mM $[K^+]_o$ depolarized astrocytes by ~20 mV, from an average of -72.9 ± 2.1 mV to -52.0 ± 2.9 mV (Fig. 1E, n = 10, inset is a representative example). These data are consistent with Ba^{2+}-sensitive K_{ir} channels contributing substantially to the resting K^+ conductance and establishment of the cells hyperpolarized RMP.

K_{ir} Channel Subunits in Spinal Cord Astrocytes

To delineate the possible candidate genes that may contribute to K_{ir} currents and the resting potassium conductance in SCA, we next examined subunit expression by PCR. We performed RT-PCR with specific primers for K_{ir} channel subunits (*Kcnj1—Kcnj16*) using mRNA from cultured SCA (>9 DIC). Table 1 summarizes the primer pairs used. When possible, we relied on previously published primer pairs. Data from three independent experiments suggest that transcripts for all known K_{ir} channel subunits were present in SCA (Fig. 2). As a negative control and to eliminate DNA as a possible source of contamination, the reverse transcription reaction was eliminated. Positive controls included probing a rat brain cDNA library in which most K_{ir} channels were cloned, with exception of $K_{ir}1.1$, for which we used a rat kidney cDNA library. The reason for the vast diversity of K_{ir} channel subunit genes expressed in astrocytes is unknown; however, these data correlate well with previous PCR studies in glial cells, demonstrating the expression of multiple K_{ir} channel subunits (Raap et al., 2000; Schroder et al., 2000).

Biophysical and Pharmacological Properties of Astrocytic K_{ir} Currents Suggest That Currents Are Mediated by $K_{ir}4.1$

We next employed biophysical and pharmacological techniques in an attempt to identify the K_{ir} subunit responsible for inward currents in SCA. Although all K_{ir} channels give rise to inwardly rectifying currents, the degree of rectification differs among them: $K_{ir}2.x$ and 3.x subfamily members do not pass any appreciable outward current and thus have strongly rectifying currents. In contrast, $K_{ir}1.x$ and 4.x subunits permit outward current and are termed weakly rectifying currents (Nichols and Lopatin, 1997). A typical voltage-ramp recording (inset) from a cultured SC shown in Figure 3A demonstrates an I-V curve with weak inward rectification, i.e., with a significant contribution of outward currents. Accordingly, both inward and outward components of this current are blocked by Ba^{2+} (Fig. 3A, bottom). For comparison, we include a recording that we obtained from a microglial cell showing strong inwardly rectifying Ba^{2+}-sensitive K_{ir} currents (Fig. 3B). In contrast to SCA, only the inward current is inhibited by Ba^{2+} application in microglial cells (Fig. 3B, bottom). Microglial cells are known to express strongly inwardly rectifying currents that are mediated by genes of the $K_{ir}2.x$ subfamily (Kettenmann et al., 1993; Eder, 1998).

Unfortunately, specific inhibitors for subtypes of K_{ir} channels are few. However, a limited pharmacological delineation of K_{ir} channels is possible using two inhibitors: tertiapin and tolbutamide. Tertiapin is a short peptide isolated from honeybee venom that has been shown to block $K_{ir}1.1$ and $K_{ir}3.1/3.4$ channels at a concentration of 10 nM (Jin and Lu, 1998). Tolbutamide selectively inhibits $K_{ir}6.x$ channels. Blockade of glial inwardly rectifying currents by tolbutamide (100 and 500 μM) has been documented for rat Bergmann glial cells (Thomzig et al., 2001), frog retinal Müller cells (Skatchkov et al., 2002), and complex glial cells from rat hippocampus (Burg, 2000). Extracellular application of tolbutamide (100 μM) to cultured SCA in the absence of ATP did not show any significant inhibition (Fig 4A, n = 7). Similarly, when increased to higher concentrations of tolbutamide (500 μM), no significant inhibition was observed (data not shown, n = 6). $K_{ir}6.x$ channels are ATP-sensitive, in that intracellular

NIH-PA Author Manuscript

NIH-PA Author Manuscript

NIH-PA Author Manuscript

ATP inhibits channel activity. These studies were carried out in the absence of ATP, a condition required for the activation of K_{ir}6.x channels. We also observe K_{ir} channel activity when ATP is added to the internal solution (Bordey and Sontheimer 2000). The lack of an ATP-sensitive current, as well as the insensitivity to tolbutemide would suggest that if K_{ir}6.x channels are present, they are not active in SCA. Furthermore, the small decrease of inward currents by tertiapin from 97.7 ± 17.9 pA to 85.5 ± 15.3 pA was not statistically significant (Fig. 4B, n = 6, $P > 0.05$).

The biophysical and pharmacological data demonstrate that K_{ir} currents in SCA are weakly rectifying and tolbutamide and tertiapin insensitive. Although we cannot rule out the possibility of unique heteromeric channels in SCA, the data presented essentially rule out a contribution of several homomeric K_{ir} channels, including K_{ir}1.1 or the 2.x, 3.x, and 6.x subfamily members. However, the properties of K_{ir} currents in SCA are similar to those described for K_{ir}4.1. Indeed, K_{ir}4.1 is the most studied inward rectifier in glial cells in the central nervous system, and K_{ir}4.1 mRNA and protein have been identified in the rat spinal cord (Poopalasundaram et al., 2000).

Molecular Characterization of K_{ir} Channel Subunits in Spinal Cord Astrocytes

RT-PCR data demonstrated that the K_{ir}4.1 subunit (*Kcnj10*) is expressed in SCA (Fig. 2). Often gene expression does not translate into protein expression. To determine whether K_{ir}4.1 may be the protein mediating astrocytic K_{ir} currents, we investigated K_{ir}4.1 protein expression by Western blot (Fig. 5A). Blots containing lysates from differentiated (9 DIC) cultured rat spinal cord (SC) and cortical (CTX) astrocytes were probed with K_{ir}4.1-specific antibodies. Human embryonic kidney cells (HEK) cells served as a negative control on the same blot. The blot was stripped and re-probed with actin as a loading control. The resulting Western blots demonstrate prominent expression of K_{ir}4.1 is in both spinal cord and cortical cultured astrocytes. The band at ~50 kD represents the monomer while the 200 kD band is thought to represent a tetramer. We presume the band at 100 kD to be nonspecific binding as it is also present in the HEK cell lane.

For K_{ir}4.1 to contribute to measurable K^+ currents, channels should localize primarily to the plasma membrane. This is indeed the case as judged by immunocytochemical labeling of cells with K_{ir}4.1 antibodies. Figure 5B is a representative example of an astrocyte immunostained for K_{ir}4.1 (green) and the astrocyte-specific cytsoskeletal protein GFAP (red). The merged digital confocal image demonstrates punctate K_{ir}4.1 immunoreactivity covering the entire surface of the cell, including the very fine distal processes. The staining pattern of cytoskeletal GFAP is quite distinct from that of K_{ir}4.1 as readily visible in the unmerged images (Fig. 5B, top).

The data presented thus far suggest that K_{ir}4.1 protein is expressed in SCA at the cell membrane. However, to identify this subunit unequivocally as being responsible for currents in SCA, we next turned to approaches that specifically allow the elimination or suppression of this gene. In the first series of experiments, we used a shRNA construct to interfere with the expression of K_{ir}4.1 in SCA. We used a K_{ir}4.1 knockout mouse in a second approach.

K_{ir}4.1 shRNA Reduces K_{ir} Channel Activity in Spinal Cord Astrocytes

We transfected SCA with an EGFP expressing plasmid containing a short hairpin RNA (shRNA) construct directed against K_{ir}4.1 (pK_{ir}4.1-OFF EGFP) at the time of the dissection (P0). The plasmid offers an advantage over traditional siRNAs in that it continually produces the short hairpin sequence as long as the cells are cultured. With traditional siRNAs, the cells would have to be continually treated throughout the 10–12 days of culturing. Sister cultures transfected with just the plasmid containing the GFP (pZOFF EGFP) served as a negative

NIH-PA Author Manuscript

NIH-PA Author Manuscript

NIH-PA Author Manuscript

control for these experiments. A biophysical comparison was made at 8–10 DIV by recording from the shRNA treated cells as compared to control cells. Transfected cells were identified under the microscope by their fluorescence at the time of the recording. A representative voltage ramp is shown in Figure 6A. Mean current density data demonstrate a significant difference in current amplitude between the mock transfected (pZOFF EGFP) and $pK_{ir}4.1$-OFF EGFP-transfected cells (Fig. 6B, 148 ± 29 n = 11, 44.2 ± 14 pA/pF, n = 10, respectively). No difference in cell size was observed between the pZOFF EGFP and $pK_{ir}4.1$-OFF EGFP astrocytes. We would like to note that included in the mean data of 10 $pK_{ir}4.1$-OFF EGFP cells are three cells that did have Ba^{2+} sensitive K_{ir} currents, while the other seven lacked any appreciable inward current. We presume this is due to an incomplete knockdown as the current in these cells appears identical to those in mock transfected cells. In contrast, all 11 of the mock transfected cells showed large K_{ir} currents. Mean RMP values were significantly more depolarized in $pK_{ir}4.1$-OFF EGFP transfected cells compared to mock transfected cells (Fig. 6C, -48.3 ± 2.6 mV, n = 11 and -67 mV ± 0.9 mV, n = 13, respectively). Finally, the input resistance, was significantly higher in $pK_{ir}4.1$-OFF EGFP transfected cells when compared to control cells (Fig. 6D, 89 ± 14 MΩ, n = 11 and 37 ± 4 MΩ, n = 13, respectively) as would be expected from cells containing fewer K^+ channels contributing to the resting conductance. These data suggest that in cultured SCA, the inward current responsible for the majority of the cells resting conductance and the maintenance of the RMP is, at least in large part, mediated by $K_{ir}4.1$.

Spinal Cord Astrocytes From $K_{ir}4.1$ Knockout Mice Lack K_{ir} Channels

To strengthen the argument that $K_{ir}4.1$ is the principle K_{ir} channel in SCA, we established a breeding colony of $K_{ir}4.1$ knockout mice. On the day of birth, offspring were genotyped by tail snip PCR allowing us to establish SC astrocyte cultures from knockout and wild-type animals (Fig. 7A). We were able to demonstrate elimination of $K_{ir}4.1$ protein by Western blot (Fig. 7B). This blot contains cultured mouse cortical astrocytes from the control (WT), heterozygous (HTZ) and $K_{ir}4.1$ knockout (KO) animals from two independent dissections as well as a comparison with rat spinal cord (SC) astrocytes. We next compared electrophysiological properties from the wild-type and knockout mice. Recordings from SCA obtained from wild-type mice were indistinguishable from those isolated from rats. However, recordings from the knockout mice (Fig. 8A,B) showed little evidence for any inward K^+ current and this was true for all SCA studied. For a quantitative comparison we calculated the peak current density (at -140 mV) of the astrocytic inward current of the wild-type (33.8 ± 6.4 pA/pF, n = 14) and knockout animals (9.6 ± 1.2 pA/pF, n = 14; Fig. 8C). Once again, no difference in cell size was observed. This was done without subtracting leakage currents therefore the remaining current in the KO may well represent leakage currents. We would like to note that included in the mean WT current density data, three cells expressed very small inward currents (<20 pA/pF). These data clearly illustrate that $K_{ir}4.1$ is the major K_{ir} channel in SCA. Indeed, the $K_{ir}4.1$ knockout recordings are reminiscent of recordings we have previously shown in immature SCA, which show an almost complete lack of inward current and large outwardly rectifying currents (MacFarlane and Sontheimer 2000,Olsen and Sontheimer 2004b). In agreement with previously published data from Müller cells (Kofuji et al., 2000) we demonstrate that the $K_{ir}4.1$ knockout animals have a significantly more depolarized RMP than the wild-type animals (-41 ± 1 mV n = 15, and -54.8 ± 2.9 mV n = 15, respectively; Fig. 8D), as well as a significantly higher input resistance (642 ± 54 MΩ n = 14 and 142 ± 45 MΩ n = 14, respectively; Fig. 8E).

K_{ir} Channel Expression In Vivo

We next examined the expression of K_{ir} channels in the whole spinal cord to validate our findings in cultured astrocytes. First, $K_{ir}4.1$ protein expression in the whole spinal cord was

NIH-PA Author Manuscript

NIH-PA Author Manuscript

NIH-PA Author Manuscript

examined by Western blot. $K_{ir}4.1$ immunoreactivity in astrocytes from fixed sections was investigated. Finally, we obtained recordings from astrocytes in acute slices from rat.

We probed Western blots containing lysates of whole spinal cord from rats at P0, P15 and P30 (Fig. 9). We observed bands at ~50 and 200 kD, similar to the observed in cultured cells. Interestingly, $K_{ir}4.1$ immunoreactivity showed a strong developmental upregulation whereby protein levels increase with postnatal development. This correlates well with the developmental upregulation of K_{ir} channel activity seen in astrocytes both in vivo and in vitro (Ransom and Sontheimer, 1995;Bringmann et al., 1999; Bringmann et al., 2000; MacFarlane and Sontheimer 2000).

Our next objective was to demonstrate $K_{ir}4.1$ expression in astrocytes of the whole spinal cord. Cervical, thoracic and lumbar slices (50 μm) of paraformaldehyde perfused rats (P15—P20) were immunostained. Results from four independent experiments indicate that $K_{ir}4.1$ was consistently expressed and predominately labeled the gray matter (outlined in white) in each spinal cord section, although some labeling in the white matter was also visible (Fig. 10A). Figure 10A demonstrates that throughout the regions we investigated there was a consistent labeling pattern with more pronounced labeling at the ventral horn, with a decrease in staining toward the dorsal horn (arrow). To ensure astrocyte-specific expression in these experiments, we co-immunostained cells with antibodies to the Na^+-dependent glutamate transporter GLT-1 (Fig. 10B). Results from these experiments suggest that $K_{ir}4.1$ and GLT-1 largely overlap throughout the gray matter (see merged panel), with a decrease in expression in the apex of the dorsal horn or substantia gelatinosa (Fig. 10B, arrow, middle). Immunoreactivity from astrocytes of the dorsal corticospinal tract exhibited very weak $K_{ir}4.1$ staining (compare first and second images at arrowhead, Fig. 10B). Our data demonstrate that there is no overlap or co-localization between the neuronal marker Neu-N with $K_{ir}4.1$, suggesting that $K_{ir}4.1$ does not label neurons in the spinal cord slice (Fig. 10C). Furthermore, $K_{ir}4.1$ and the oligodendrocyte marker, myelin basic protein, demonstrated very little overlap in either the white or the gray matter (Fig. 10D). In the last panel of Figure 10E, a higher magnification of $K_{ir}4.1$ and GLT-1 demonstrates overlap of these two proteins in the ventral horn of the spinal cord.

Finally, to correlate $K_{ir}4.1$ protein expression in spinal cord slices with measurable K_{ir} currents, we obtained electrophysiological recordings in spinal cord slices. Due to the decrease in immunoreactivity we observed towards the apex of the dorsal horn, we avoided this region in our recordings and instead made recordings in other regions of the gray matter. Figure 10 shows representative whole-cell patch clamp recordings from astrocytes stimulated with either voltage-ramp (Fig. 11A) or voltage step (Fig. 11B) protocols. As in cultured cells, we saw weak inwardly rectifying current that demonstrated a characteristic inactivation at negative potentials (Fig. 11B). These weakly rectifying currents were completely inhibited by 100 μM Ba^{2+} (Fig. 11A, bottom). Astrocytes in slices typically had low input resistance values, often as low as 20 MΩ and had mean RMP values of 74.0 ± 0.96 mV (n = 23). Thus, the electrophysiological profile of astrocytic inward currents in cultured cells appeared similar to those in spinal cord slices.

DISCUSSION

Little doubt remains that astrocytes have a high K^+ permeability and that this feature is a requirement for potassium buffering in brain. This resting K^+ permeability is also responsible for establishing the hyperpolarized membrane potential that has become a hallmark feature of astrocytes. However, except in Müller cells, the identity of the underlying K^+ channels is unknown. The data we present in this study answer this question for SCA as well. Our data show that SCA express $K_{ir}4.1$, a weakly rectifying K_{ir} channel. To demonstrate this in rat,

NIH-PA Author Manuscript

NIH-PA Author Manuscript

NIH-PA Author Manuscript

which has been the model system for 15 years, we used shRNA which eliminated Ba^{2+}-sensitive currents. We then turned to the $K_{ir}4.1$ knockout mouse to directly compare cultured SCA in both rat and mouse. Importantly, the shRNA data in rat astrocytes and knockout data from the mouse converge and demonstrate a lack of inward current, depolarized RMPs, and higher input resistances in these astrocytes.

Although a great deal of attention has focused on the expression of $K_{ir}4.1$ in astrocytes, multiple K_{ir} gene transcripts and subunits have been identified in astrocytes from different brain regions. For example, $K_{ir}4.1$ transcripts and protein have been shown to be expressed in mouse astrocytes where the protein appears to colocalize with GFAP-positive stellate and protoplasmic astrocytes in brain (Li et al., 2001). In primary cultured Müller cells from guinea pig mRNA for $K_{ir}2.1$, 2.2, 2.4, 3.1, 3.2, 4.1, and 6.1 was shown to be expressed (Raap et al., 2002). Other mammalian Müller cells express protein for $K_{ir}5.1$ (Ishii et al., 2003). Moreover, in situ single cell RT-PCR experiments identified $K_{ir}2.1$, 2.2, 2.3 and 4.1 in hippocampal astrocytes (Schroder et al., 2002). We now expanded this screen to include probes for all known K_{ir} channel subunits and found an even greater diversity of K_{ir} channel transcripts present in SCA. The reason for the vast diversity of K_{ir} channel subunit genes expressed in astrocytes is unknown. In light of the abundance of subunits found in astrocytes, one would have expected that $K_{ir}4.1$ may be one of many contributors to the overall astrocytic K^+ conductance. In fact one would have expected that knockdown of $K_{ir}4.1$ may lead to the compensatory upregulation of other K_{ir} genes. Yet by contrast, our studies suggest that both in rat and mouse spinal cord $K_{ir}4.1$ is the principle subunit expressed. It is possible that astrocytic K_{ir} channels are formed by the heteromeric association of multiple K_{ir} genes, and hence the disruption of $K_{ir}4.1$ may be sufficient to eliminate functional channels. A heteromeric assembly from $K_{ir}4.1$ and 5.1 has been shown for astrocytes in neocortex and in the glomeruli of the olfactory bulb (Hibino et al., 2004). This question certainly merits further study.

It is also important to emphasize that astrocytes from different brain regions may express different K_{ir} genes and $K_{ir}4.1$ may only be expressed in a subset. Immunohistochemical studies suggest that only a limited population of brain astrocytes express $K_{ir}4.1$ (Higashi et al., 2001), whereas our immunochemistry results from rat spinal cord suggests that the vast majority of astrocytes in the spinal cord express $K_{ir}4.1$. This variable expression may be related to functional differences between astrocytes from different brain regions.

An important point made in this study is that $K_{ir}4.1$ is the channel that establishes a hyperpolarized membrane potential in SCA. A role for $K_{ir}4.1$ in contributing to the resting potential may indeed be as important as its role as a potential pathway for K^+ uptake. Numerous transport systems, including those for neurotransmitters and glucose, use the Na^+ gradient across the astrocytic membrane as energy source. Hence, the more negative the astrocytic membrane potential, the greater their ability to uptake substrate from the extracellular space. This may be particularly relevant with regard to glutamate uptake via the EAAT family of electrogenic, Na^+-dependent transporters (Danbolt, 2001). Indeed, it would be worthwhile to compare the ability of astrocytes from $K_{ir}4.1$ knockout animals directly to wild-type animals to establish such a role for $K_{ir}4.1$.

An interesting observation from our Western blot analysis is a profound developmental upregulation of $K_{ir}4.1$ in whole spinal cord. This finding correlates well with our previous reports on a developmental increase in K_{ir} channel activity in SCA (Ransom and Sontheimer, 1995; MacFarlane and Sontheimer, 2000; Olsen and Sontheimer, 2004b). In fact, a positive correlation between K_{ir} channel activity and glial cell maturation or differentiation has been shown repeatedly in glial cells from in vitro ands in situ studies (Kressin et al., 1995; Bordey and Sontheimer, 1997; Bringmann et al., 1999; MacFarlane and Sontheimer, 2000). We propose that $K_{ir}4.1$ is primarily responsible for establishing a hyperpolarized RMP in astrocytes

NIH-PA Author Manuscript

NIH-PA Author Manuscript

NIH-PA Author Manuscript

to aid cells in their various uptake processes. Upon expression of $K_{ir}4.1$, astrocytes could be considered differentiated and probably have associated with blood vessels on which they form endfeet (Nagelhus et al., 2004) and/or have invested processes around synapses where they maintain transmitter homeostasis (Lehre et al., 1995).

ACKNOWLEDGMENTS

The authors thank Dr. W. Joon Chung for his valuable contribution constructing the modified shRNA plasmid.

Grant sponsor: National Institutes of Health; Grant number: RO1-NS36692; Grant number: RO1-NS31234; Grant number: 2 P30 HD 038985.

REFERENCES

Bordey A, Lyons SA, Hablitz JJ, Sontheimer H. Electrophysiological characteristics of reactive astrocytes in experimental cortical dysplasia. J Neurophysiol 2001;85:1719–1731. [PubMed: 11287494]

Bordey A, Sontheimer H. Postnatal development of ionic currents in rat hippocampal astrocytes in situ. J Neurophysiol 1997;78:461–477. [PubMed: 9242294]

Bordey A, Sontheimer H. Passive glial cells, fact or artifact? J Membr Biol 1998a;166:213–222. [PubMed: 9843595]

Bordey A, Sontheimer H. Properties of human glial cells associated with epileptic seizure foci. Epilepsy Res 1998b;32:286–303. [PubMed: 9761328]

Bordey A, Sontheimer H. ion channel expression by astrocytes in situ: comparison of different CNS regions. Glia 2000;30:27–38. [PubMed: 10696142]

Bringmann A, Biedermann B, Reichenbach A. Expression of potassium channels during postnatal differentiation of rabbit Müller glial cells. Eur J Neurosci 1999;11:2883–2896. [PubMed: 10457185]

Burg MB. Macromolecular crowding as a cell volume sensor. Cell Physiol Biochem 2000;10:251–256. [PubMed: 11125203]

Coetzee WA, Amarillo Y, Chiu J, Chow A, Lau D, McCormack T, Moreno H, Nadal MS, Ozaita A, Pountney D, Saganich M, Vega-Saenz dM, Rudy B. Molecular diversity of K^+ channels. Ann NY Acad Sci 1999;868:233–285. [PubMed: 10414301]

Danbolt NC. Glutamate uptake. Prog Neurobiol 2001;65:1–105. [PubMed: 11369436]

Eder C. Ion channels in microglia. brain macrophages. Am J Physiol 1998;275:C327–342. [PubMed: 9688586]

Guatteo E, Stanness KA, Janigro D. Hyperpolarization-activated ion currents in cultured rat cortical and spinal cord astrocytes. Glia 1996;16:196–209. [PubMed: 8833190]

Hagiwara S, Takahashi K. The anomalous rectification and cation selectivity of the membrane of a starfish egg cell. J Membr Biol 1974;18:61–80. [PubMed: 4854650]

Hamill OP, Marty A, Neher E, Sakmann B, Sigworth FJ. Improved patch-clamp techniques for high-resolution current recording from cells and cell-free membrane patches. Pflugers Arch 1981;391:85–100. [PubMed: 6270629]

Hibino H, Fujita A, Iwai K, Yamada M, Kurachi Y. Differential assembly of inwardly rectifying K^+ channel subunits, $K_{ir}4.1$ and $K_{ir}5.1$, in brain astrocytes. J Biol Chem 2004;279:44065–44073. [PubMed: 15310750]

Higashi K, Fujita A, Inanobe A, Tanemoto M, Doi K, Kubo T, Kurachi Y. An inwardly rectifying K^+ channel, $K_{ir}4.1$, expressed in astrocytes surrounds synapses and blood vessels in brain. Am J Physiol Cell Physiol 2001;281:C922–C931. [PubMed: 11502569]

Jin W, Lu Z. A novel high-affinity inhibitor for inward-rectifier K^+ channels. Biochem 1998;37:13291–13299. [PubMed: 9748337]

Kettenmann H, Banati R, Walz W. Electrophysiological behavior of microglia. Glia 1993;7:93–101. [PubMed: 7678582]

Kofuji P, Ceelen P, Zahs KR, Surbeck LW, Lester HA, Newman EA. Genetic inactivation of an inwardly rectifying potassium channel. $K_{ir}4.1$ subunit. in mice: phenotypic impact in retina. J Neurosci 2000;20:5733–5740. [PubMed: 10908613]

NIH-PA Author Manuscript

NIH-PA Author Manuscript

NIH-PA Author Manuscript

Kressin K, Kuprijanova E, Jabs R, Seifert G, Steinhäuser C. Developmental regulation of Na^+ and K^+ conductances in glial cells of mouse hippocampal brain slices. Glia 1995;15:173–187. [PubMed: 8567069]

Kuffler SW. Neuroglial cells: physiological properties and a potassium mediated effect of neuronal activity on the glial membrane potential. Proc R Soc Lond B Biol Sci 1967;168:1–21. [PubMed: 4382871]

Kuffler SW, Potter DD. Glia in the leech central nervous system: physiological properties and neuron-glia relationship. J Neurophysiol 1964;27:290–320. [PubMed: 14129773]

Lehre KP, Levy LM, Ottersen OP, Storm-Mathisen J, Danbolt NC. Differential expression of two glial glutamate transporters in the rat brain: quantitative and immunocytochemical observations. J Neurosci 1995;15:1835–1853. [PubMed: 7891138]

Li L, Head V, Timpe LC. Identification of an inward rectifier potassium channel gene expressed in mouse cortical astrocytes. Glia 2001;33:57–71. [PubMed: 11169792]

MacFarlane SN, Sontheimer H. Electrophysiological changes that accompany reactive gliosis in vitro. J Neurosci 1997;17:7316–7329. [PubMed: 9295378]

MacFarlane SN, Sontheimer H. Changes in ion channel expression accompany cell cycle progression of spinal cord astrocytes. Glia 2000;30:39–48. [PubMed: 10696143]

Marcus DC, Wu T, Wangemann P, Kofuji P. KCNJ10. K_{ir}4.1. potassium channel knockout abolishes endocochlear potential. Am J Physiol Cell Physiol 2002;282:C403–C407. [PubMed: 11788352]

Nagelhus EA, Mathiisen TM, Ottersen OP. Aquaporin-4 in the central nervous system: cellular and subcellular distribution and coexpression with KIR4.1. Neuroscience 2004;129:905–913. [PubMed: 15561407]

Neusch C, Rozengurt N, Jacobs RE, Lester HA, Kofuji P. K_{ir}4.1 potassium channel subunit is crucial for oligodendrocyte development and in vivo myelination. J Neurosci 2001;21:5429–5438. [PubMed: 11466414]

Newman EA. Regional specialisation of retinal glial cell membrane. Nature 1984;309:155–157. [PubMed: 6717594]

Newman EA. Membrane physiology of retinal glial. Müller. cells. J Neurosci 1985;5:2225–2239.

Newman EA. Inward-rectifying potassium channels in retinal glial. Müller. cells. J Neurosci 1993;13:3333–3345.

Nichols CG, Lopatin AN. Inward rectifier potassium channels. Annu Rev Physiol 1997;59:171–191. [PubMed: 9074760]

Olsen, ML.; Sontheimer, H. Voltage-activated ion channels in glial cells. In: Ransom, BR.; Kettenmann, H., editors. Neuroglia. 2nd. Oxford University Press; New York: 2004. p. 112-130.

Olsen ML, Sontheimer H. Mislocalization of K_{ir} channels in malignant glia. Glia 2004b;46:63–73. [PubMed: 14999814]

Orkand RK, Nicholls JG, Kuffler SW. Effect of nerve impulses on the membrane potential of glial cells in the central nervous system of amphibia. J Neurophysiol 1966;29:788–806. [PubMed: 5966435]

Poopalasundaram S, Knott C, Shamotienko OG, Foran PG, Dolly JO, Ghiani CA, Gallo V, Wilkin GP. Glial heterogeneity in expression of the inwardly rectifying K^+ channel, K_{ir}4.1, in adult rat CNS. Glia 2000;30:362–372. [PubMed: 10797616]

Ransom BR, Goldring S. Ionic determinants of membrane potential of cells presumed to be glia in cerebral cortex of cat. J Neurophysiol 1973;36:855–868. [PubMed: 4805015]

Ransom CB, Sontheimer H. Biophysical and pharmacological characterization of inwardly rectifying K^+ currents in rat spinal cord astrocytes. J Neurophysiol 1995;73:333–345. [PubMed: 7714576]

Ransom CB, Sontheimer H, Janigro D. Astrocytic inwardly rectifying potassium currents are dependent on external sodium ions. J Neurophysiol 1996;76:626–630. [PubMed: 8836250]

Sakmann B, Trube G. Conductance properties of single inwardly rectifying potassium channels in ventricular cells from guinea-pig heart. J Physiol Lond 1984;347:641–657. [PubMed: 6323703]

Schroder W, Seifert G, Huttmann K, Hinterkeuser S, Steinhauser C. AMPA receptor-mediated modulation of inward rectifier K^+ channels in astrocytes of mouse hippocampus. Mol Cell Neurosci 2002;19:447–458. [PubMed: 11906215]

NIH-PA Author Manuscript

NIH-PA Author Manuscript

NIH-PA Author Manuscript

Skatchkov SN, Rojas L, Eaton MJ, Orkand RK, Biedermann B, Bringmann A, Pannicke T, Veh RW, Reichenbach A. Functional expression of K_{ir} 6.1/SUR1-KATP. channels in frog retinal Müller glial cells. Glia 2002;38:256–267. [PubMed: 11968063]

Sykova E. Modulation of spinal cord transmission by changes in extracellular K^+ activity and extracellular volume. Can J Physiol Pharmacol 1987;65:1058–1066. [PubMed: 3621032]

Terry-Lorenzo RT, Roadcap DW, Otsuka T, Blanpied TA, Zamorano PL, Garner CC, Shenolikar S, Ehlers MD. Neurabin/protein phosphatase-1 complex regulates dendritic spine morphogenesis and maturation. Mol Biol Cell 2005;16:2349–2362. [PubMed: 15743906]

Thomzig A, Wenzel M, Karschin C, Eaton MJ, Skatchkov SN, Karschin A, Veh RW. K_{ir}6.1 is the principal pore-forming subunit of astrocyte but not neuronal plasma membrane K-ATP channels. Mol Cell Neurosci 2001;18:671–690. [PubMed: 11749042]

NIH-PA Author Manuscript
NIH-PA Author Manuscript
NIH-PA Author Manuscript

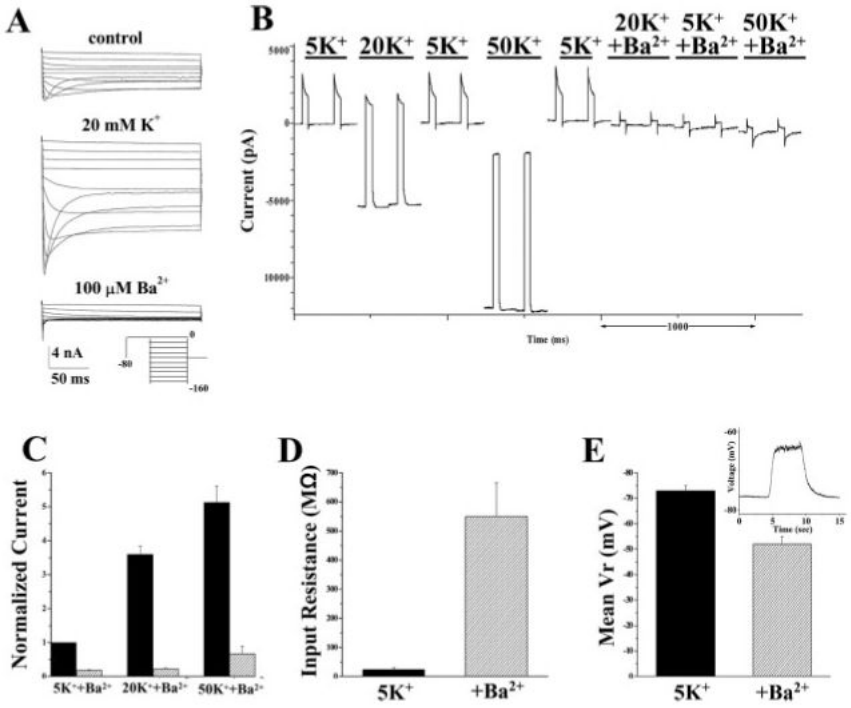

Fig. 1.

K_{ir} currents contribute to the resting conductance in SCA. **A:** Typical voltage-step response (protocol depicted in inset) in 5 mM $[K^+]_o$ (top), 20 mM $[K^+]_o$. (middle), and 5 mM $[K^+]_o$ + 100 μM Ba^{2+} (bottom). **B:** Small voltage steps (-80 to -40 mV, ~5 Hz) in SCA elicits a robust current, which is potentiated in 20 mM and 50 mM extracellular potassium ($[K^+]_o$) and inhibited by Ba^{2+} application. There is also a shift in holding current in increased $[K^+]_o$, both of which return to baseline when returned to control conditions. **C:** Current amplitude increased to nearly five-fold of control in 50 mM $[K^+]_o$, while >90% of the current at each $[K^+]_o$ concentration is inhibited by Ba^{2+} (n = 5). **D:** Input resistance increased dramatically in the presence of bath applied Ba^{2+} from a mean value of 24.2 ± 7.9 mΩ to 549.5 ± 116.6 MΩ (n = 4). **E:** Current clamp experiments demonstrated that application of Ba^{2+} depolarized SCA by ~20 mV (n = 10, inset shows a representative example).

NIH-PA Author Manuscript

NIH-PA Author Manuscript

NIH-PA Author Manuscript

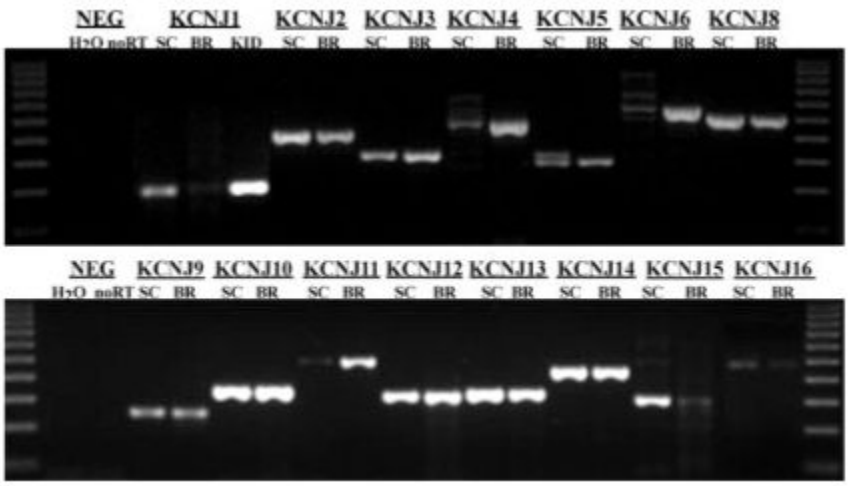

Fig. 2.

Reverse transcription polymerase chain reaction (RT-PCR) experiments in SCA demonstrated positive expression for all K_{ir} genes examined. The first and last lanes gel are a 100-bp marker, the second and third lanes are negative controls with water being substituted for mRNA and next, no reverse transcription reaction, respectively. For all negative controls, the *Kcnj10* primers were used. In each subsequent lane, the primers for the designated gene were used first in SCA (>9 DIC) and then a rat brain cDNA library was used as a positive control. Low detection levels of *Kcnj1* in the rat brain prompted us to test a rat kidney (KID) cDNA library as well. The primer pairs and the expected molecular weight of each product are summarized in Table 1.

NIH-PA Author Manuscript

NIH-PA Author Manuscript

NIH-PA Author Manuscript

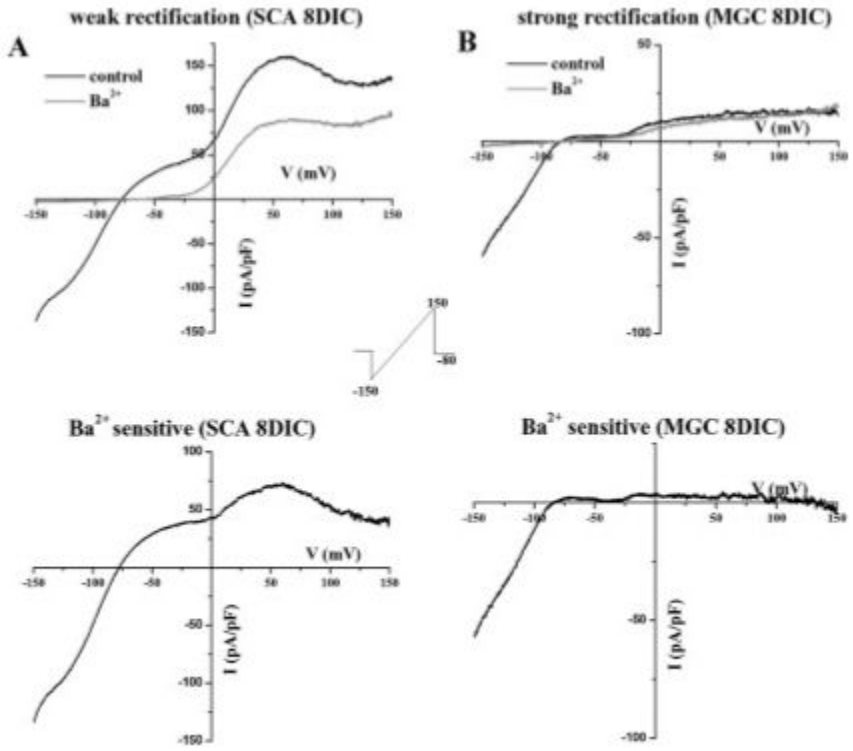

Fig. 3.

K_{ir} channels in SCA were weakly rectifying. **A:** Typical current response elicited from a linear voltage ramp (protocol depicted in inset) in SCA (8 DIC) demonstrates that Ba^{2+} inhibits a significant current at positive and negative potentials surrounding the reversal potential. The subtracted barium sensitive current is weakly rectifying (bottom). **B:** In contrast, Ba^{2+} inhibited only inward K_{ir} currents in microglial cells (MGC, 8 DIC), indicating these were strongly rectifying. The subtracted barium sensitive current was strongly rectifying (B, bottom).

NIH-PA Author Manuscript

NIH-PA Author Manuscript

NIH-PA Author Manuscript

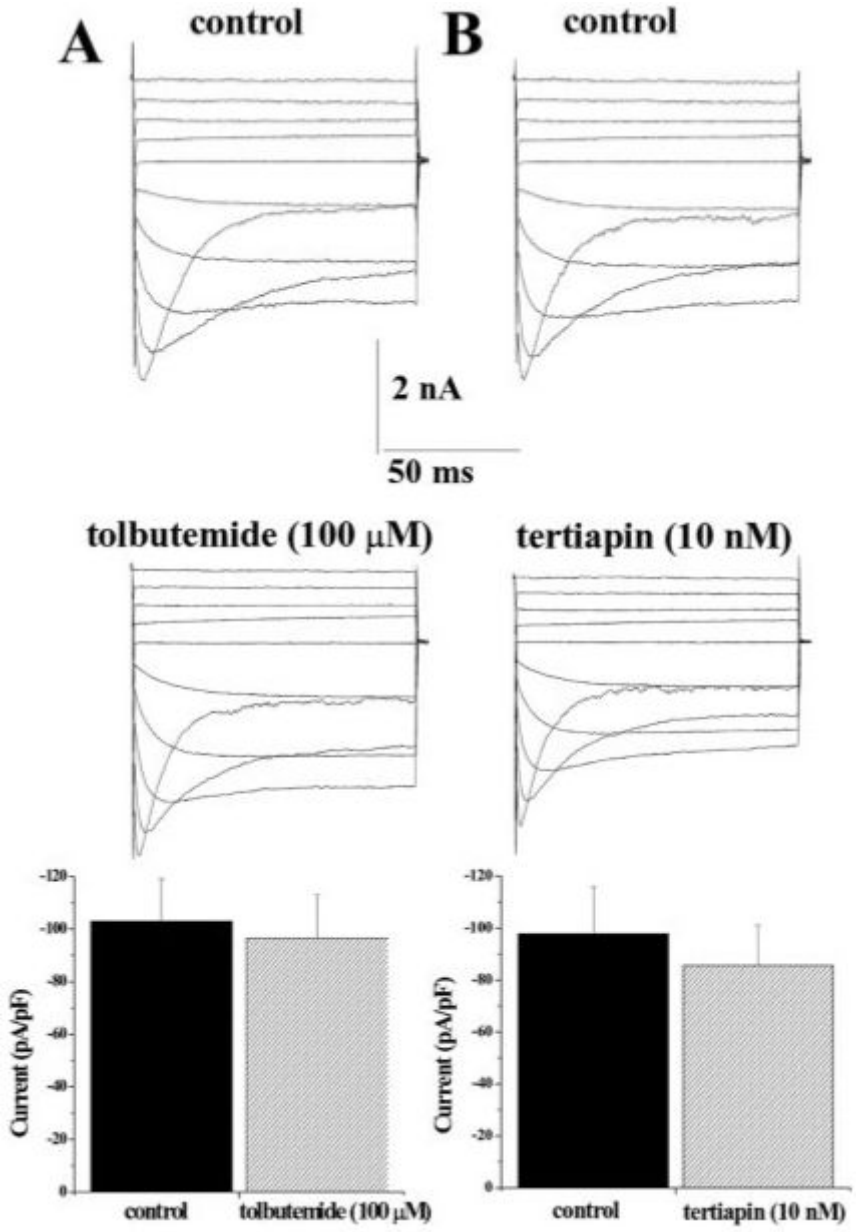

Fig. 4.

K_{ir} currents in SCA are tolbutamide and tertiapin insensitive. **A:** Typical voltage-step and mean data (peak current density plotted at -140 mV) before and after tolbutamide (100 μM, 103.0 ± 16.0 pA/pF to 96.7 ± 16.2 pA/pF, respectively, n = 6) indicated that SCA are insensitive to tolbutamide. **B:** Similarly, tertiapin. (10 nM) had an insignificant effect on K_{ir} currents from SCA (n = 6).

NIH-PA Author Manuscript

NIH-PA Author Manuscript

NIH-PA Author Manuscript

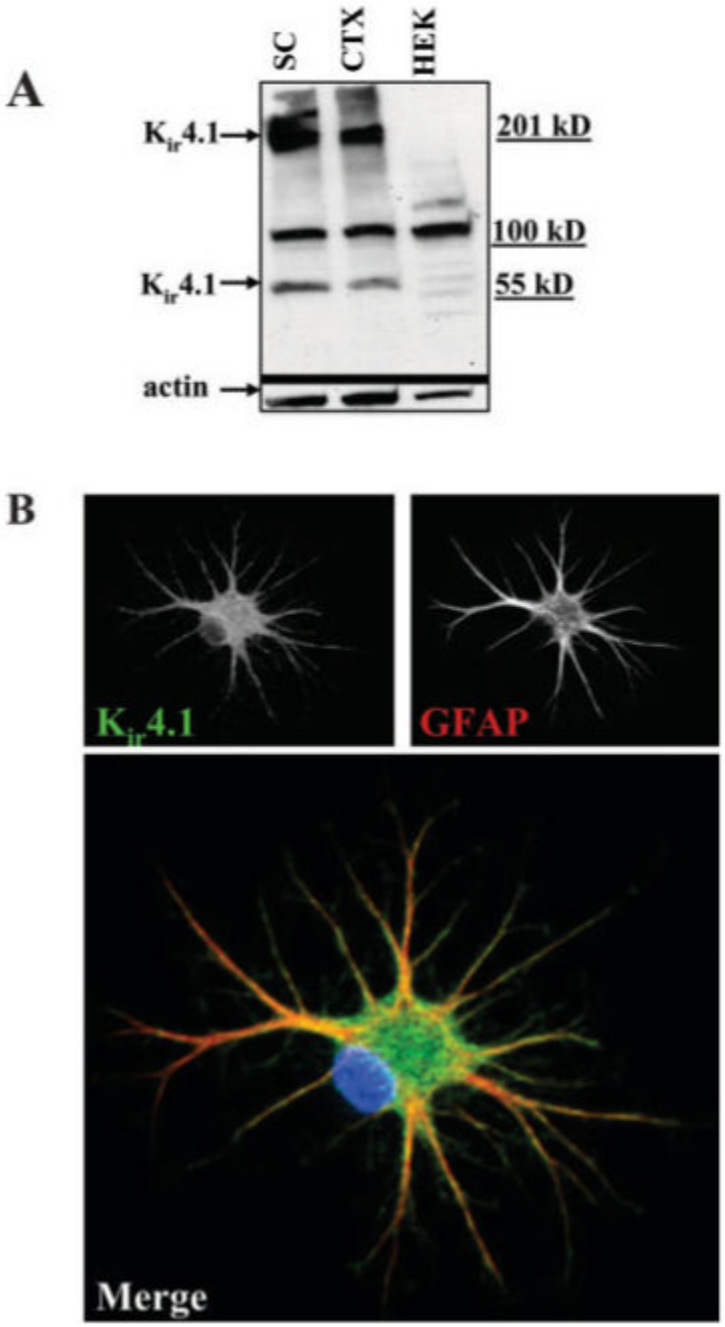

Fig. 5.

K_{ir}4.1 protein is expressed in cultured SCA. **A:** Western blot of cultured spinal cord (SC) and cortical (CTX) astrocytes (9 DIC) is shown. HEK cells were used as a negative control. This blot was stripped and re-probed with actin as a loading control. Bands at ~50 and 200 kD represent K_{ir}4.1 monomer and tetramers. **B:** Immunocytochemistry revealed surface localization of K_{ir}4.1 in cultured SCA. Anti-GFAP is used to co-label and indicated astrocytes. The color image on the bottom is a merged K_{ir}4.1 (green) and GFAP (red) image. DAPI stain is in blue. Scale bar = 20 μm.

NIH-PA Author Manuscript

NIH-PA Author Manuscript

NIH-PA Author Manuscript

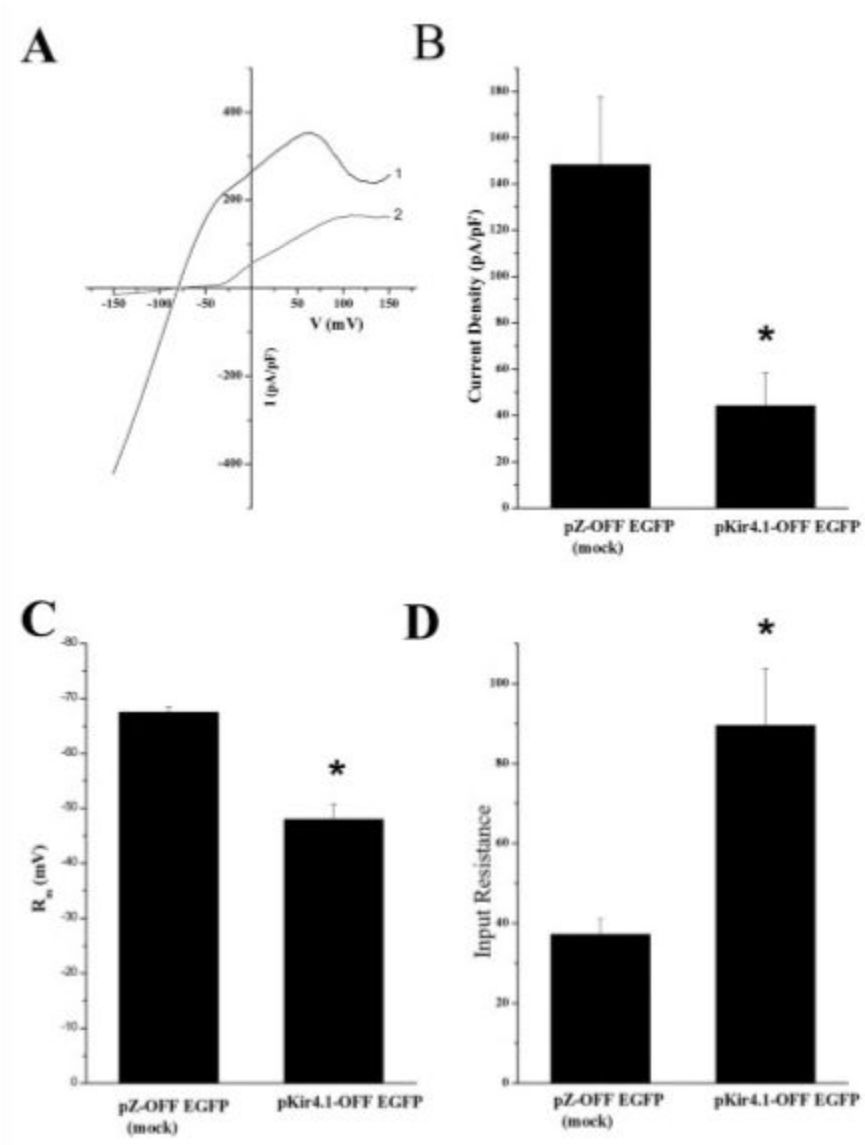

Fig. 6.

K_{ir}4.1 shRNAs knockdown spinal cord astrocyte inwardly rectifying currents. **A:** Representative voltage ramp from pZOFF EGFP (1,black) and pK_{ir}4.1-OFF EGFP (2, gray) transfected are shown. **B:** Mean current density data from mock and pK_{ir}4.1-OFF EGFP transfected cells demonstrated a significant difference in current amplitude (peak current at -140 mV, mock n = 13, K_{ir}4.1shRNA, n = 11, $P < 0.05$). **C:** Bar graph summarizing resting membrane potentials in pZOFF EGFP and pK_{ir}4.1-OFF EGFP transfected cells. mock n = 13, K_{ir}4.1shRNA, n = 11, $P < 0.05$). D: This bar graph represents summary data of input resistance values in pZOFF EGFP and pK_{ir}4.1-OFF EGFP transfected cells (mock n = 13, K_{ir}4.1shRNA, n = 11, $P < 0.05$).

NIH-PA Author Manuscript
NIH-PA Author Manuscript
NIH-PA Author Manuscript

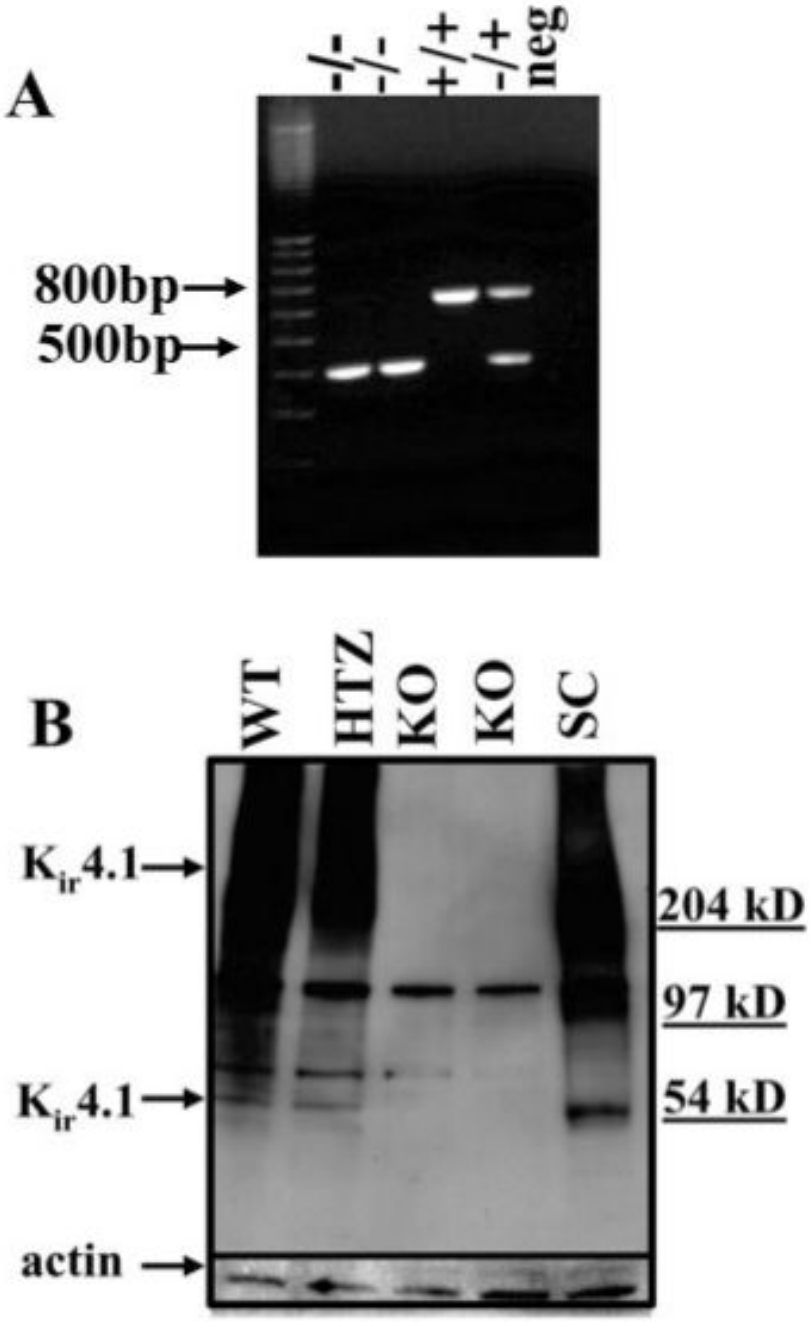

Fig. 7.

Littermates were genotyped before establishing astrocytic cultures for $K_{ir}4.1$ protein analysis. **A:** Mice were genotyped by tail snip PCR to distinguish wild-type, heterozygous and $K_{ir}4.1$ knockout animals. From the left to right, 100-bp DNA ladder, two $K_{ir}4.1$ knockout animals (-/- allele has 383-bp band), wild-type (WT) (+/+ allele only has 634 bp), heterozygous (+/- allele has both bands) and last lane, absence of mouse genomic DNA (no band). **B:** Western blot of cultured astrocytes from control and knockout animals demonstrates $K_{ir}4.1$ expression. **Lane 1**, WT cultured cortical astrocytes; **lane 2**, heterozygous cultured cortical astrocytes; **lanes 3,4**, cultured cortical astrocytes from 2 knockout animals; **lane 5**, rat spinal cord lysates used as a positive control. This blot was stripped and reprobed with actin as a loading control.

NIH-PA Author Manuscript

NIH-PA Author Manuscript

NIH-PA Author Manuscript

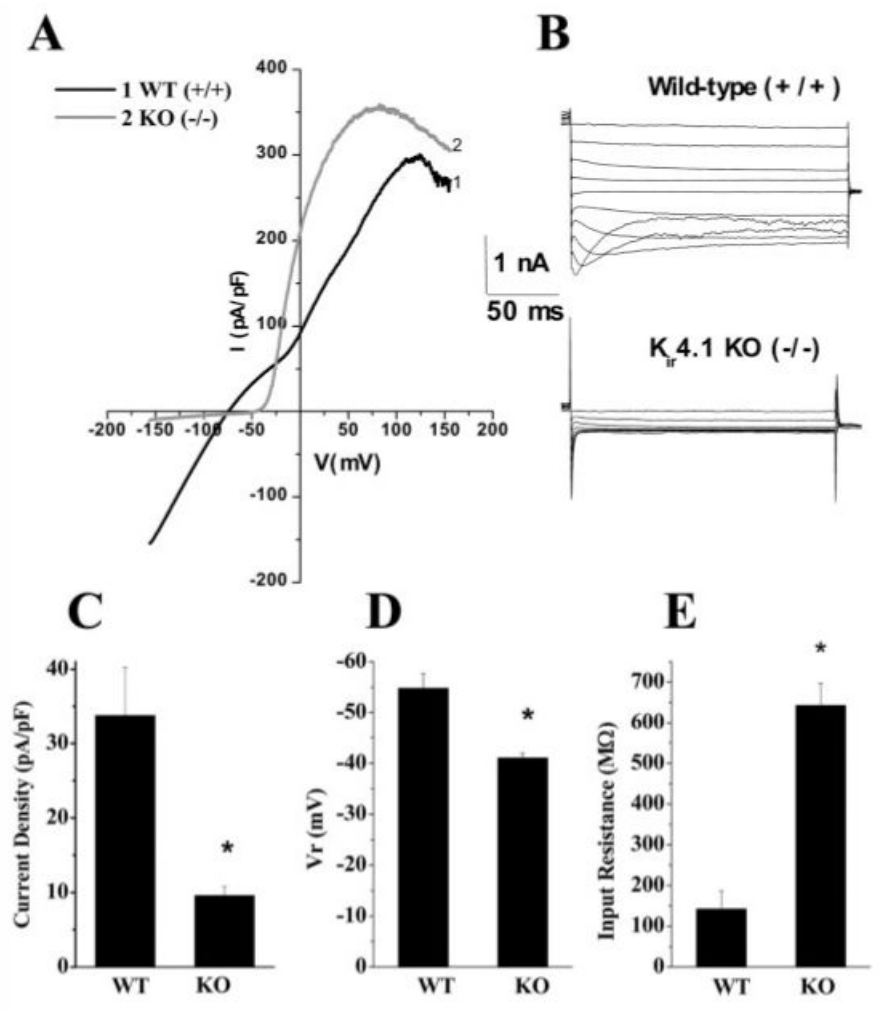

Fig. 8.

Spinal cord inwardly rectifying K_{ir} currents were absent in K_{ir}4.1 knockout mice. **A:** Trace showing a representative example of whole-cell currents elicited by a linear voltage-ramp from the wild-type (+/+) and the K_{ir}4.1 (-/-) knockout mouse. **B:** Traces showing representative voltage steps before and after application of Ba^{2+} (100 μM). **C:** Bar graph representing summary current density data. pA/pF) from wild-type and knockout mice. Wild-type (WT), n = 14; KO n = 14, $P < 0.05$). **D:** Bar graph representing mean resting membrane potential values in wild-type and K_{ir}4.1 knockout mice (WT, n = 15; KO, n = 15, $P < 0.05$). **E:** Bar graph representing summary data of input resistance values in the wild-type and K_{ir}4.1 knockout mice (WT, n = 14; KO, n = 14, $P < 0.05$).

NIH-PA Author Manuscript

NIH-PA Author Manuscript

NIH-PA Author Manuscript

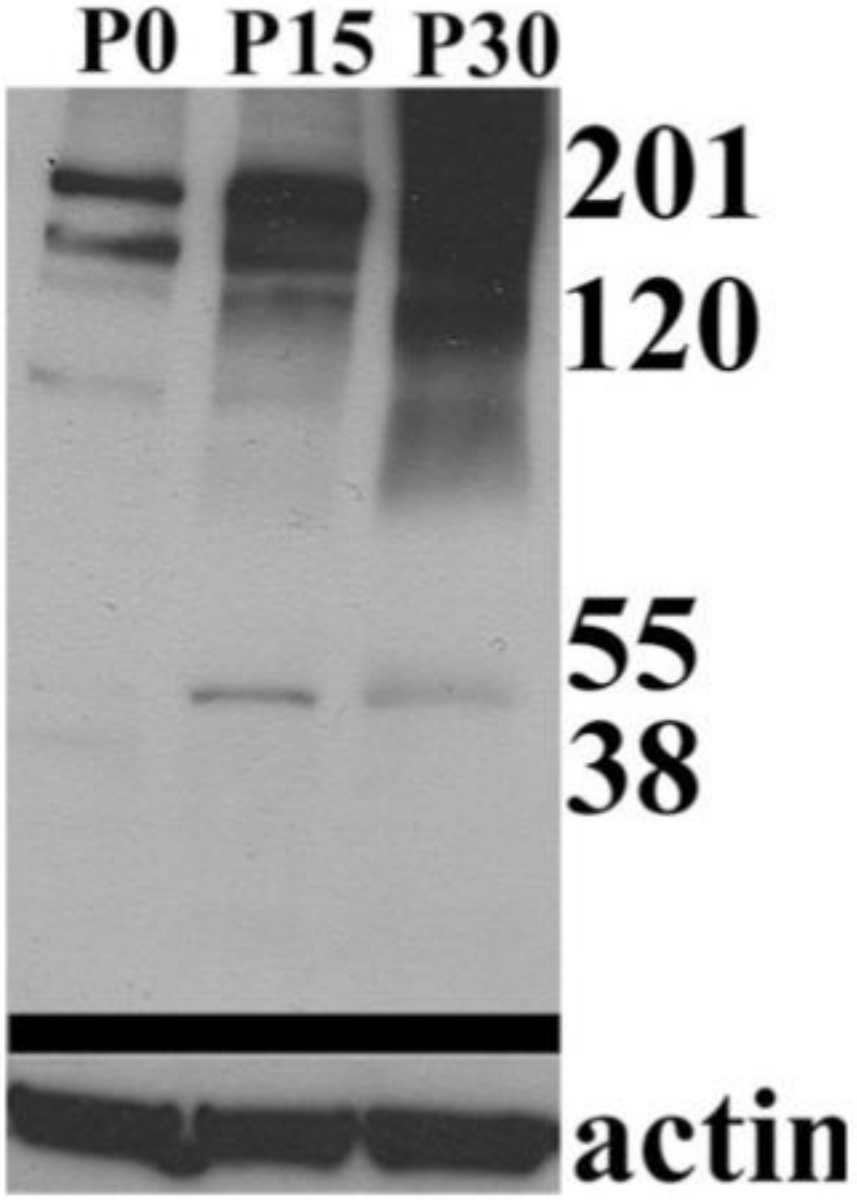

Fig. 9.

Western blot of rat spinal cord demonstrated developmental upregulation of $K_{ir}4.1$. $K_{ir}4.1$ immunoreactivity in rat spinal cord at P0, P15 and P30 shows a strong developmental upregulation ($K_{ir}4.1$ bands at ~ 50 and 200 kD). This blot was stripped and re-probed using actin as a loading control.

NIH-PA Author Manuscript
NIH-PA Author Manuscript
NIH-PA Author Manuscript

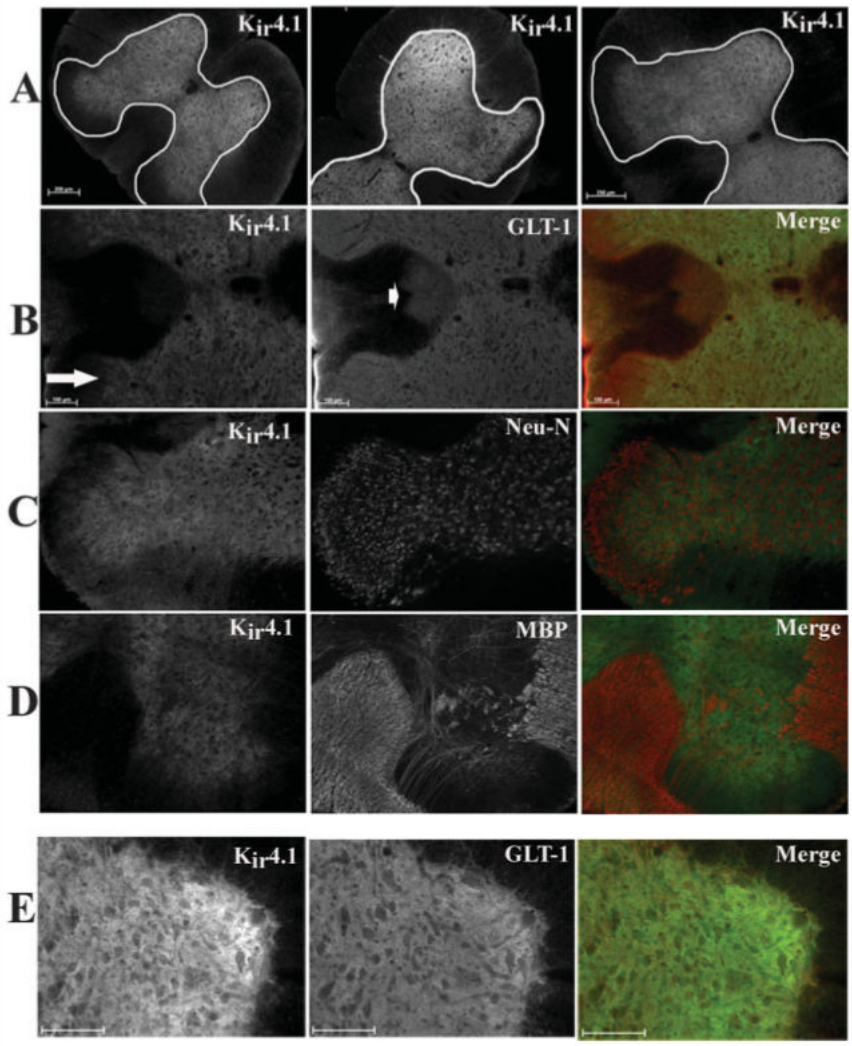

Fig. 10.

Immunohistochemistry demonstrated $K_{ir}4.1$ is prominently expressed in the gray matter astrocytes in spinal cord in vivo. All images were from fixed, 50-μm sections from the cervical, lumbar, and thoracic regions. **A:** K_{ir} 4.1 is expressed throughout the gray matter in each spinal cord section (scale bar 250 μm). **B:** $K_{ir}4.1$ and GLT-1 (an astrocyte-specific glutamate transporter) largely overlap in the gray matter, however, GLT-1-positive cells in the apex of the dorsal horn (arrow) and astrocytes in the dorsal corticospinal tracks (arrowhead) that demonstrated very little $K_{ir}4.1$ immunoreactivity. **C:** $K_{ir}4.1$ and Neu-N (a neuronal marker) did not demonstrate similar staining patterns in the spinal cord slice. **D:** $K_{ir}4.1$ and MBP (myelin basic protein) an oligodendrocyte-specific marker, demonstrate very little overlap in either the white matter or gray matter in vivo. **E:** Higher-magnification image of $K_{ir}4.1$ and GLT-1 demonstrate overlap of the two proteins in the spinal cord slice. Scale bar = 100 μm in B,E.

NIH-PA Author Manuscript
NIH-PA Author Manuscript
NIH-PA Author Manuscript

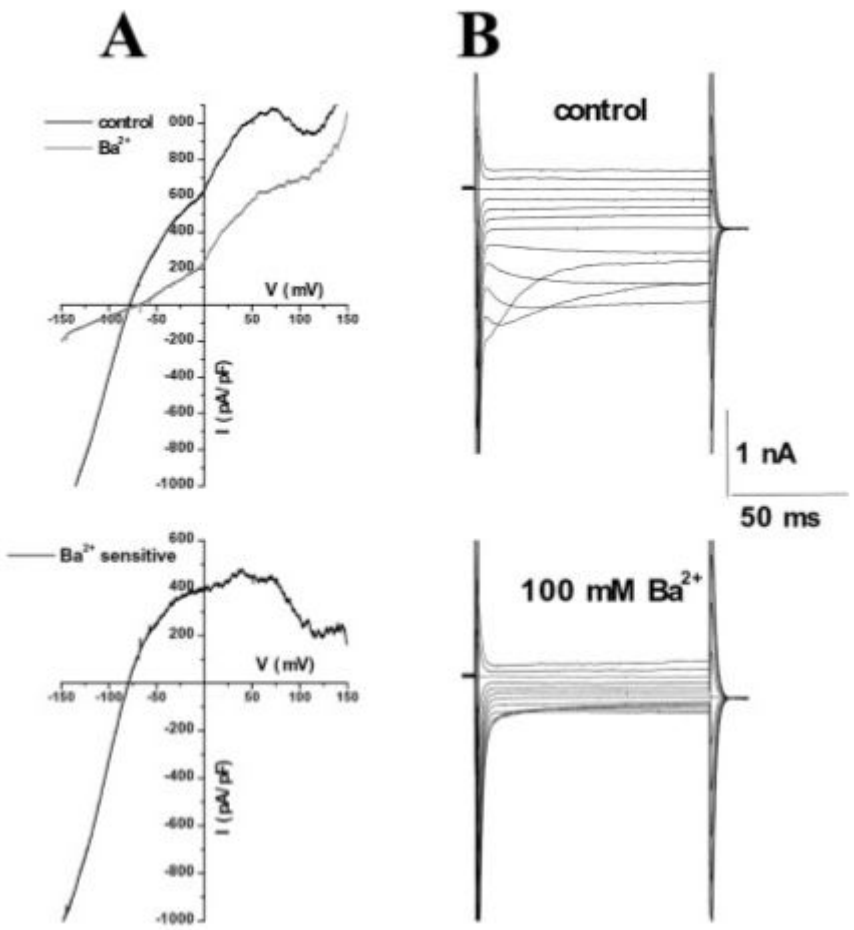

Fig. 11.

Electrophysiology from astrocytes in situ revealed similar inward currents as those seen in cultured cells. **A:** Trace showing a representative example of whole-cell currents elicited by a linear voltage-ramp from P15 rat spinal cord slice before and after application of Ba^{2+}. The subtracted barium sensitive current is weakly rectifying (A, bottom). **B:** Traces showing representative voltage steps before and after application of Ba^{2+} (100 μM).

NIH-PA Author Manuscript
NIH-PA Author Manuscript
NIH-PA Author Manuscript

TABLE 1

Primer Sets Used to RT-PCR K_{ir} Genes From Spinal Cord Astrocytes

Gene	Protein	Accession No.	Primer pairs	BP
Kcnj1	K_{ir}1.1/Romk	NM_017023	GGGCACTGACAGAAAGGATG CCTCCATTTCAGGTCCAG (Li et al., 2001)	197
Kcnj2	K_{ir}2.1	NM_017296	GAGTAAGCAGGACATTGACAATG GATTCTCGCCTTAAAGGCCT	429
Kcnj3	K_{ir}3.1/Girk1	NM_031610	TCCATCGAAGCTGCAGAAAATTACG TGCCTAATGGGGTGTTTTGCTATGT	329
Kcnj4	K_{ir}2.3	NM_053870	GCATGGGCAAGGAGGAACTGGAGTC CTTGCATGCGCTCCAGATCCAGGT	471
Kcnj5	K_{ir}3.4/Girk 4	NM_017297	AGATGTCTCGTGCTCAACTGGA GGAGGACTGGGCAAGGACTGGA	289
Kcnj6	K_{ir}3.2/Girk2	NM_013192	CCCAGTGGCCATTCACCAGC GTGGGTGGAAAAGACCAGGG (Raap et al., 2002)	559
Kcnj8	K_{ir}6.1	NM_017099	AATCCCATCGAGAGCCAATAACA GTTTCCTTCTGGAGTCATGAAT	501
Kcnj9	K_{ir}3.3/Girk 3	NM_053834	CCCGCCTTGACGCCCATCTCTA TGCCTGCCTCCTCTACTTCCAT	247
Kcnj10	K_{ir}4.1	NM_031602	GCAAGATCTCCCCCTCCGCAG CAGACGTTACTAATGCGCACACT	345
Kcnj11	K_{ir}6.2	NM_031358	ACCCTCATCTTCAGCAAGCA GTGGGCACTTTAACGGTGTT (Raap et al., 2002)	486
Kcnj12	K_{ir}2.2	NM_053981	AGCCTTCCTGAGCCGAGATGAG AATCCACCCTCCTGCCAACTTT	313
Kcnj13	K_{ir}7.1	NM_053608	CCTGCTCCAGCATGAGACTCCTTC GTCTTATTCTGTCAGCCCTGTTTC	322
Kcnj14	K_{ir}2.4	NM_170718	CGCATCTTCCTCGTATCCCCCATTA CTTCTTCATCTTCCTCCTGGCAGC	423
Kcnj15	K_{ir}4.2	NM_133321	GGACCTCACACCCCAGAACCTA CACGTTCCCTCTGGTCCTCCTG	296
Kcnj16	K_{ir}5.1	NM_053314	CGGTGAGAGCCCAACTTCTGCG TGGTGTCCGAGGTGCAGGATCC	462